Superacid-assisted Degradation of Polystyrene

Atharwa Thigale,[†] *Carrie Trant,*[†] *Juhong Ahn,*[†] *Melissa Nelson,*[†] *Chang Y. Ryu,*[‡] *Chulsung Bae,*[†,‡] *Sangwoo Lee*,*[†]

[†]Department of Chemical and Biological Engineering, Rensselaer Polytechnic Institute, Troy, NY.

[‡]Department of Chemistry and Chemical Biology, Rensselaer Polytechnic Institute, Troy, NY.

[*]Corresponding Author: lees27@rpi.edu

KEYWORDS: Polystyrene Upcycling, Polystyrene Degradation, Superacid, Chain coupling, Polycyclic aromatic hydrocarbons

TOC Graphic (For Table of Contents Use Only) -

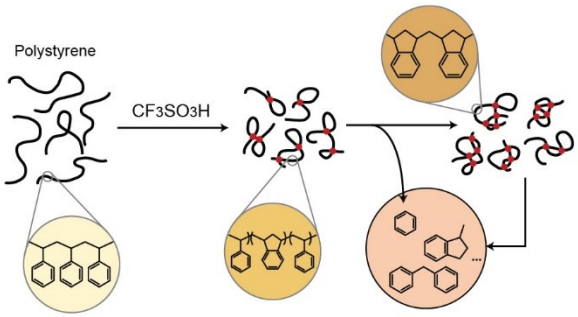

ABSTRACT

We report the degradation pathway of polystyrene in a low-temperature environment by superacid. Polystyrene is a thermoplastic resin widely used for packaging, disposable products, and structural materials. However, economically viable upcycling of polystyrene has yet to be established because of the high cost of chemical recycling and the low value of products. To understand the degradation pathway of polystyrene and establish competitive upcycling practices, we investigated the transformation of normal and deuterated polystyrene chains into small compounds by triflic acid at 20 °C. The degradation study of deuterated polystyrene showed the high stability of the hydrogens at the α carbons of polymerized styrene against triflic acid, which suggests the known β-scission degradation pathway of polystyrene by α-proton abstraction is unlikely. Rather, the polystyrene degradation proceeds through three distinct stages: i) *intra*-chain crosslinking that forms polymer nanoparticles and simultaneous transformation of polymerized styrene to indan units, ii) degradation of the polymer nanoparticles into small molecular weight compounds, and iii) formation of polycyclic aromatic hydrocarbons. The stepwise degradation pathway of polystyrene we report may enable the design of efficient and profitable upcycling processes for end-of-life polystyrene products in low-temperature environments.

Introduction

Polystyrene (PS) is a thermoplastic produced by more than 25 million metric tons per year, approximately 6 % of the total polymers annually produced worldwide, and proportionally occupies a similar fraction (~ 5.6%) in the total plastic waste collected.[1] PS is transparent, glossy, hard, chemically and thermally inert, and stable in biological environments. The material and processing costs of PS are low, particularly for expanded forms.[2-6] Those material properties and low material and processing cost make PS an excellent thermoplastic resin as a packaging material, building and construction component, matrix polymer of composites, and beyond.[7] However, compared to other high-volume plastic resins such as polyethylene and polyethylene terephthalate, PS in the stream of end-of-life plastic waste is relatively small, and the cost of sorting and recycling PS products does not meet the economy of scales. Furthermore, PS is often copolymerized or blended with other polymers and components for improved mechanical properties such as impact resistance. For example, styrene-butadiene rubbers and many high-performance PS-based materials have been developed and established stable market shares.[8] However, because of their low values and high processing costs, the multi-component PS products are difficult to be included in the circular economy of plastics unless a universal and cost-competitive method of chemical upcycling is established.

So far, various recycling strategies for PS products have been explored. Mechanical recycling of PS has been documented, but this strategy generally requires mixing end-of-life PS with virgin materials and results in downgraded resins for limited applications, like other mechanically recycled plastics.[9-13]

Chemical recycling of PS has been pursued primarily using pyrolytic and catalytic methods. Pyrolysis of PS recovers a relatively large amount of styrene monomer by depolymerization, but

the high ceiling temperature of PS ($T_{ceiling,PS}$ ≈ 395 °C) requires a high energy cost processing environment. Also, other challenges, such as wax formation and thermal repolymerization, further worsen the economic validity of PS pyrolysis.[14-17] Recently, biodegradation methods of PS have been reported.[18-21] However, undesirable by-products, scalability issues, and low efficiency limit its applicability.[22, 23] Chemical recycling of PS by oxidation processes like UV-assisted photocatalysis and ozonation has been reported.[24-33] Those photocatalytic methods primarily produce oxidized phenyl compounds, but like the other methods, efficiency, cost issues, and other method-specific difficulties should be further improved. Relatively low-temperature catalytic conversion of PS, primarily using Brønsted acids (≤ 300 °C), produces phenyl hydrocarbon compounds, of which molecular weights are less than 1,000 g/mol.[34] Although the catalytic conversion of PS does not recover styrene monomer, the new hydrocarbon compounds derived from the end-of-life PS products may offer fresh opportunities for profitable and, therefore, viable economic upcycling of PS. Indeed, Xu and co-workers recently reported a tandem reaction process producing high-value diphenylmethane from PS using $AlCl_3$ and UV radiation.[35] Zhang and co-workers also described a hydrocracking method of PS using metal nitride co-doped carbon-based catalysts to produce ethylbenzene as a liquid fuel.[36]

The upcycling strategy for the value increase of end-of-life polymer products is the most promising way to build a circular plastic economy that meets profitability.[13] PS has excellent potential as a key feed stream toward viable polymer upcycling practices.[35, 36] Among chemical degradation and upcycling approaches investigated for PS, acid-assisted degradation is promising because highly reactive and cost-effective Brønsted acid reagents are available. In the earlier studies, Pukánszky and coworkers proposed a β-scission pathway activated by the deprotonation from the α-carbons of PS using $AlCl_3$.[37] Later, Nanbu and co-workers questioned this β-scission

process and proposed a different β-scission mechanism producing ω-ene and α-carbocation PS chains.[34] However, those studies are based on phenomenological observations on the reaction conditions and resultant products. It is still unclear how PS chains transform and break into small compounds for value upgrades, in particular, at economically desirable low-temperature environments.[16, 38-45] This article describes time-resolved characterizations and analysis of linear PS reacted with triflic acid at 20 °C and the degradation pathway elucidated. We observed that the degradation of PS by triflic acid proceeds in three distinct stages, i) *intra*-chain crosslinking that forms polymer nanoparticles and simultaneous transformation of PS chains to poly(styrene-*co*-indan) both initiated by removal of a phenyl group, ii) degradation of the crosslinked polymer nanoparticles into small molecular-weight compounds, and iii) formation of polycyclic aromatic hydrocarbons (PAHs). This observation suggests that the upcycling of PS proceeds in a stepwise manner that may be judiciously incorporated into a step-wise upcycling process to produce high-value compounds from end-of-life PS products.

Experimental

Materials Styrene (Acros) and *d*8-Styrene (Acros) were purified twice over *n*-butyl-*sec*-butylmagnesium (Sigma-Aldrich) at 40 °C and vacuum distilled. Cyclohexane (Sigma-Aldrich) was passed through activated alumina (BASF F-200) and copper catalyst (BASF Q-5) to remove protic and polar impurities. Triflic acid (Stream, 99+%) was used as received. $CDCl_3$ (Sigma-Aldrich) was dried using activated molecular sieves (Mallinckrodt).

Polymerization Polystyrene samples were prepared using a standard anionic polymerization technique. A typical polymerization procedure is as follows: In a dry and argon charged glass reaction vessel (2 L), dried cyclohexane (0.8 L) and *sec*-butyllithium initiator (0.12 mL of 1.4 M

solution, 1.6×10^{-4} mol) were charged. To the cyclohexane and initiator solution, purified styrene (30 g, 0.288 moles) was slowly added over three hours. The polymerization proceeded for two days at 40 °C and was terminated with degassed methanol. Polystyrene was precipitated in methanol, and the recovered polystyrene was dried under a dynamic vacuum at 150 °C.

Degradation Study A typical degradation study for the 1:1 molar ratio of styrene monomer in polystyrene and triflic acid was conducted as follows. In a 100 ml round-bottom flask immersed in a temperature-controlled water bath (20 °C), dry $CDCl_3$ (Sigma-Aldrich, 38.46 ml), polystyrene (0.5 g, 1.3×10^{-2} g/ml, 0.0048 moles in styrene monomer), and triflic acid (0.42 ml, 0.0048 moles) were added, the flask was capped with a rubber septum, and the solution was stirred.

Degradation Characterization The changes in the chemical functional groups of polystyrene reacting with triflic acid were characterized using ^{1}H NMR (Agilent 500 MHz spectrometer). The polymer and triflic acid solution (0.6 mL) was drawn from the round-bottom flask at the beginning of a degradation study, transferred to an NMR tube, and sealed. This tube was also placed in the temperature-controlled bath.

The changes in the molecular weights of polystyrene were tracked using a size exclusion chromatography system equipped with a refractive index detector (Agilent) at 30 °C. A Shodex KF-805L column was used as the stationary phase, and tetrahydrofuran as the mobile phase. Polystyrene standards (Agilent) were employed for molecular weight characterizations. Aliquots (1 ml) for the size exclusion chromatography characterizations were collected from the flask and neutralized with the saturated sodium bicarbonate solution (0.5 mL). The organic layer separated by centrifugation was analyzed. To include small molecular weight compounds in the SEC chromatograms, an aliquot sample of the separated organic layer (0.2 mL) was directly diluted with HPLC-grade tetrahydrofuran (Alfa Aesar) and analyzed.

The gas chromatography-mass spectrometry (GC-MS) characterization was employed to identify small molecular weight products (Thermo Scientific Trace 1300 GC equipped with ISQ 7000 single quadrupole MS). The GC column (TG-5SILMS) was 30 m long and 0.25 mm in diameter with 0.25 μm film thickness. For each analysis, 10 μL of each neutralized aliquot was diluted in 0.75 mL HPLC grade chloroform (Sigma-Aldrich). The GC inlet temperature was 300 °C, and the temperature of the column was ramped from 40 °C to 300 °C at a constant ramp rate of 25 °C/min. Helium at 1.5 mL/min was used as the carrier gas. The MS spectroscopy was conducted in the electron ionization (EI) mode with the ion source temperature of 310 °C and transfer line temperature of 300 °C. The total ion current (TIC) channel was used for a more inclusive mass range (m/z) analysis. The mass spectra data were processed using Chromeleon Software (Thermo Scientific). The Wiley Registry 12th edition and NIST-2020 library were used to identify the components, and the quantitative analysis of identified compounds was conducted using relative peak areas.

Results and Discussion

Three normal and one perdeuterated PS samples were anionically prepared, and the molecular weight characterization data is presented in Table 1. The number-averaged molecular weights of the normal PS samples are 34, 182, and 527 kg/mol and labeled PS-34, PS-182, and PS-527, respectively. The perdeuterated PS molecular weight is 50 kg/mol and labeled *d*8-PS-50. Those PS samples have monodisperse and narrow molecular weight distributions, of which dispersities are less than 1.2.

Table 1. Molecular weight characterization data of perdeuterated and normal polystyrene samples.

Polymer	Mn (kg/mol)	Mw (kg/mol)	Dispersity
*d*8-PS-50	50	57	1.16
PS-34	34	37	1.08
PS-182	182	196	1.08
PS-527	527	578	1.10

The protonation sites in PS chains by triflic acid were examined using the *d*8-PS-50. Three molar equivalent triflic acid (A) to the *d*8-styrene monomer polymerized (S), A:S = 3:1, was employed to induce proton-deuterium exchanges. The initial ^{1}H NMR spectrum of *d*8-PS-50 is flat due to the lack of hydrogen (the spectrum of normal PS-34 in Figure 1b is shown as a reference). In the first hour of the reaction, the ^{1}H NMR of the *d*8-PS-50 reacted with triflic acid develops a multipeak spectrum of PS, which evidences active exchanges between the deuterium of *d*8-PS-50 and the hydrogen of triflic acid. However, not all deuteriums in the *d*8-PS-50 are exchanged. The phenyl protons (D^{o}, D^{m}, D^{p}) and D^{β} at the β-carbon are exchanged with the ^{1}H of triflic acid, but the D^{α} at the α-carbon is stable (Figures 1b and 1c). The inactive D^{α} suggests that the β-scission mechanism of PS chains by the proton-activated removal of hydrogen at the α carbon proposed by Pukánszky and co-workers is not likely an active pathway.[37] Nanbu and co-workers also questioned this mechanism and suggested that another β-scission path of PS chains proceeds by the removal of proton-activated phenyl groups forming α carbenium which splits the activated PS chain into *ω*-ene- and *α*-carbocation-PS chains (Figure S1). However, our time-resolved ^{1}H NMR spectra of the *d*8-PS-50 in the first 48 hours do not show any sign of ene-functional groups (4 – 6 ppm), and the spectra with new chemical functional peaks at 48 hours and later also lack such signatures. This discrepancy is discussed below.

The exchange rates of hydrogens at the phenyl and β-carbon are different, as indicated by the normalized peak integration ratio of the $H^{o/m/p}$ and H^{β} at 1 hour is 0.28, not 1. Assuming the effective exchange energy barrier follows an Arrhenius function, the exchange energy difference between the phenyl and β hydrogens by triflic acid is $E_a(\beta) - E_a(\text{phenyl}) = -\ln(0.28)RT = 3$ kJ/mol where $R = 8.314$ $JK^{-1}mol^{-1}$ and $T = 293$ K. In contrast, the H-D exchange rates at the different phenyl group locations are the same. Although the NMR spectra reveal the active exchanges of the hydrogen atoms in the chains, the molecular weight of *d*8-PS-50 remains nearly the same for the first 12 hours. At 48 hours, the molecular weight significantly decreases to ~ 10 kg/mol, but the characteristic peak resonances of PS functional groups are almost maintained (Figure 1a and 1b). After 72 hours, the ^1H NMR spectrum records a set of new resonance peaks signaling the formation of new chemical compounds (Figure 1b).

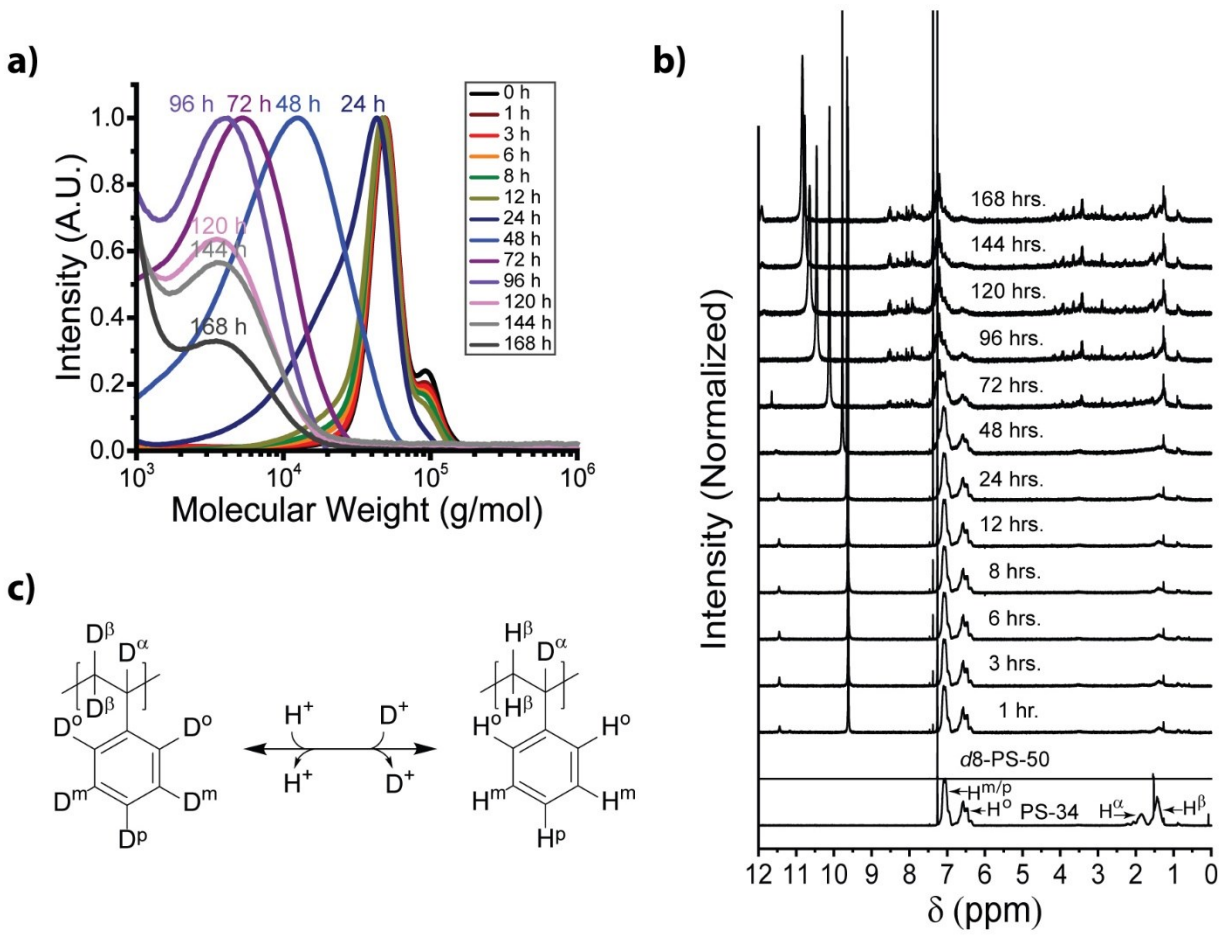

Figure 1. Time-resolved characterization results of *d*8-PS-50 reacted with 3 molar excess triflic acid to styrene monomer polymerized. (a) Time-resolved SEC chromatograms. (b) Time-resolved ^{1}H NMR spectra of *d*8-PS-50 with triflic acid. Normal PS-34 is also shown as a reference. (c) Proton-deuterium exchange sites observed from the time-resolved ^{1}H NMR. The ^{1}H NMR shows that D^{α} is inert.

We further investigated the PS degradation pathways with normal PS samples at different molar ratios of triflic acid to the styrene monomer polymerized, A:S = 0.33:1, 1:1, and 3:1. Figure 2 summarizes the time-resolved SEC chromatograms of the PS-34, PS-182, and PS-527 treated with

triflic acid. The chromatograms also include low molecular weight domains to 300g/mol based on polystyrene standards to show the intensity contribution from small molecular weight compounds formed from the PS samples (the lowest molecular weight of the polystyrene standards employed is 580 g/mol. The low molecular weight domain in SEC chromatograms generally contains the signal from uncontrolled impurities, but we observed significant intensity increase by the low-molecular weight compounds by PS degradation. See below).

At the lowest triflic acid concentration (A:S = 0.33:1), the molecular weights of the PS samples increase rather than decrease (Figure 2a, 2b, and 2c). The new molecular weight peaks, marked with arrows next to the primary peaks, are approximately double of the molecular weights of starting PS samples. This suggests that the increase of molecular weights occurs by *inter*-chain coupling. In the PS-182 and PS-527 solutions, additional high molecular weight peaks by coupling the coupled chains appear, though PS-34 only forms di-chain peaks in the same reaction hours. We attribute this molecular weight difference to the pervaded volume effect of PS chains for coupling. The coil overlap concentration, at which the polymer coils begin to contact, $c^* = 3M/\left(4\pi N_A R_g^3\right)$ where M is the molecular weight, N_A is Avogadro's number, and R_g is the radius of gyration. The overlap concentrations of PS-182 and PS-527 are calculated as $c^* \approx 3\times10^{-2}$ g/ml, close to the concentration of the PS solutions, $c = 1.3\times10^{-2}$ g/ml, i.e., those PS chains are spatially advantageous for *inter*-chain coupling. In contrast, the c^* of PS-34 is 1.8×10^{-1} g/ml, which is an order higher than the solution concentration. Despite the large molecular weight increase by *inter*-chain coupling, the ^{1}H NMR spectra of PS samples of the A:S=0.33:1 solution stay the same for the 168 reaction hours except for the decrease of the ^{1}H peak of free triflic acid at ~ 9 ppm (Figure S2).

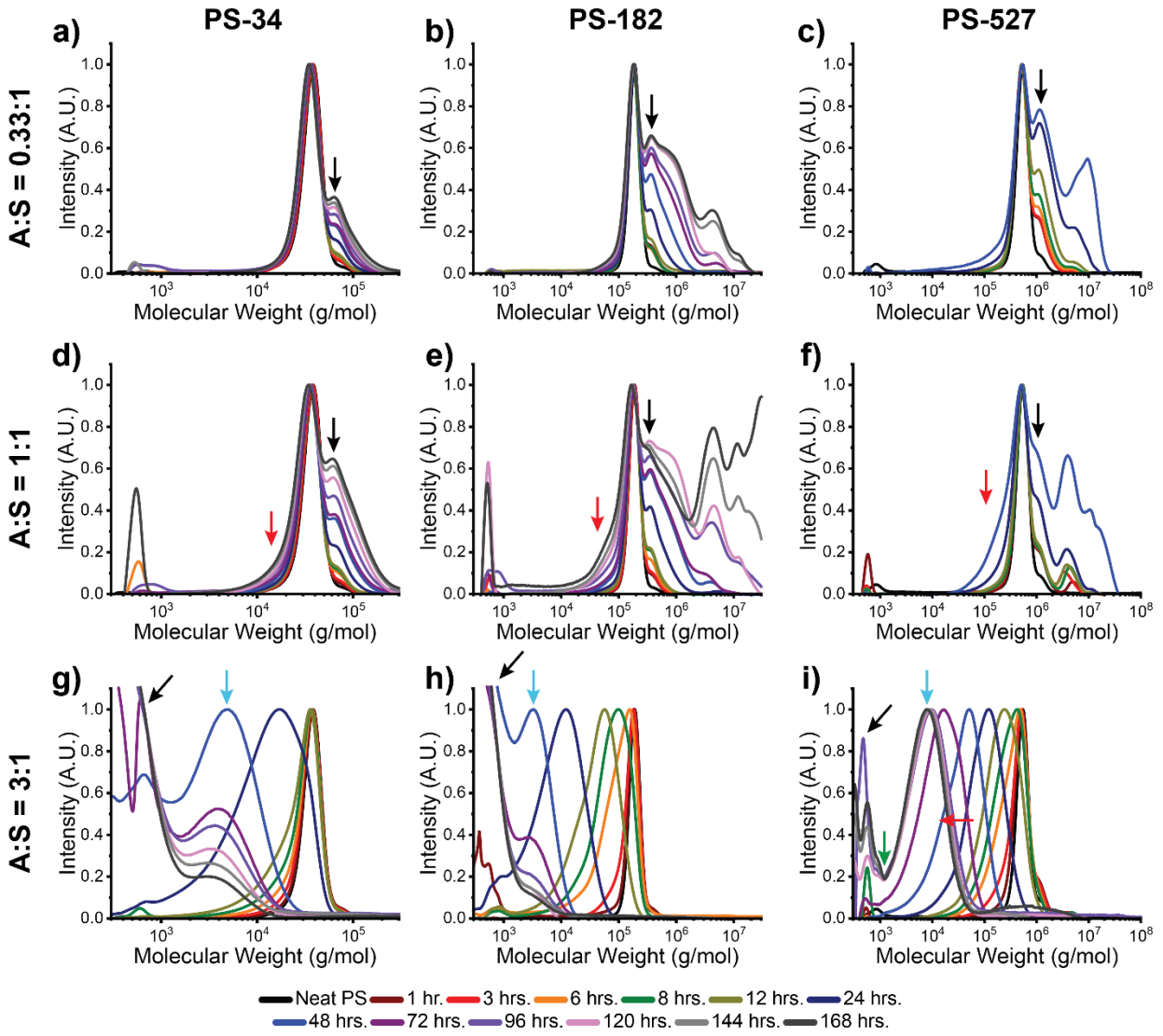

Figure 2. Time-resolved chromatograms of (a, d, and g) PS-34, (b, e, and h) PS-182, and (c, f, and i) PS-527 treated with triflic acid at the molar ratio, (a, b, and c) A:S = 0.33:1, (d, e, and f) A:S = 1:1, and (g, h, and i) A:S = 3:1. The panels in the vertical direction summarize the chromatogram profiles of a PS sample at different triflic acid concentrations over time, and the panels in the horizontal direction compare the changes in the chromatogram profiles of different PS samples at the same triflic acid concentration. Black arrows in panel a to f note the molecular weight peaks

by *inter*-chain coupling. The low molecular weight shoulders developing at the A:S = 1:1 by intra-chain couplings are indicated by red arrows in panels d to f. Blue arrows in the panels g to i indicate the nominal terminal molecular weight peaks of nanoparticles. The red arrow in panel i notes the decrease of the nominal molecular weight of nanoparticles by the hydrodynamic volume over time, and the green arrow marks the lower limit of the nominal molecular weight of nanoparticles. For details, see the text.

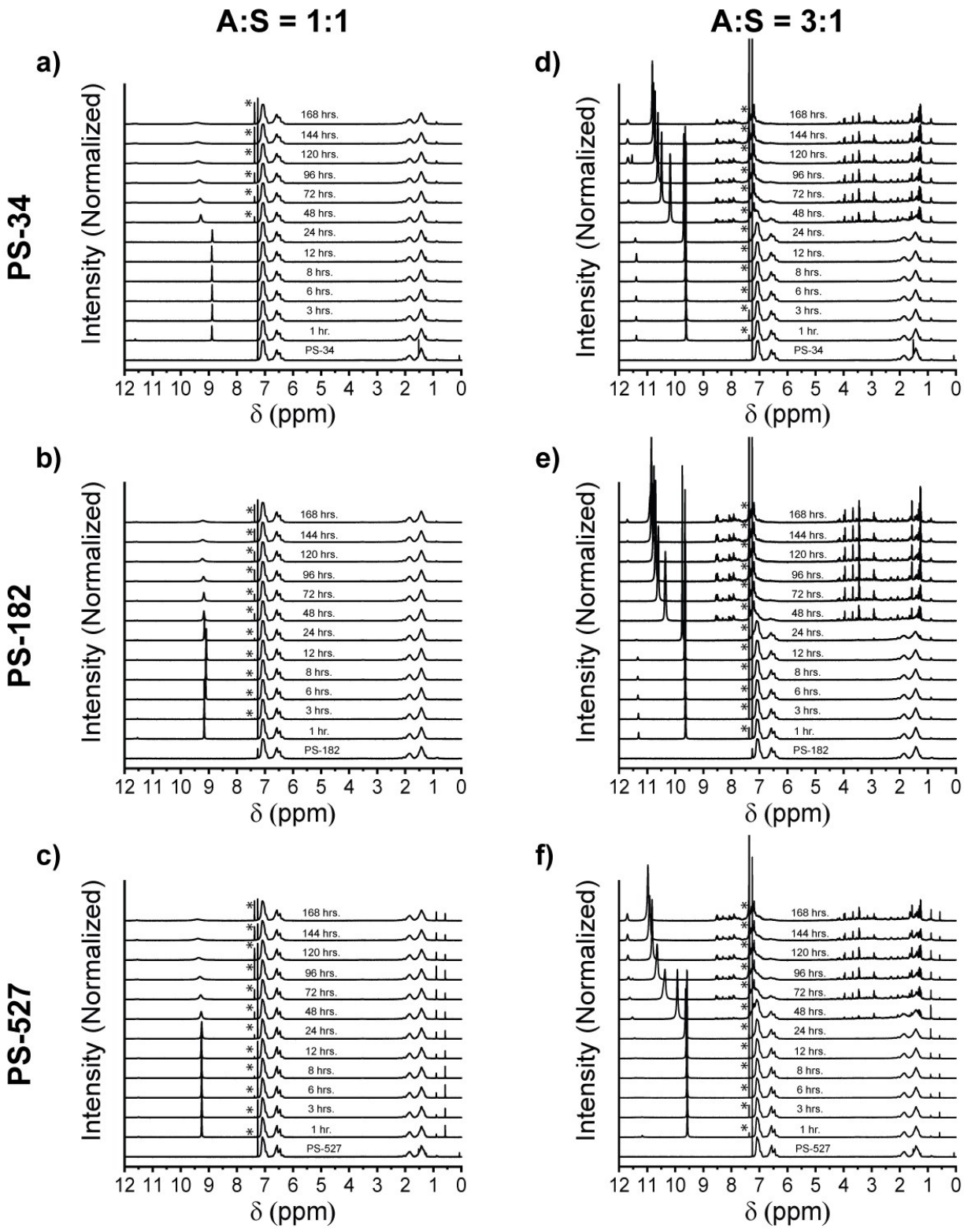
A:S = 1:1
A:S = 3:1
a)
b)
c)
d)
e)
f)
PS-34
PS-182
PS-527
Intensity (Normalized)
δ (ppm)
12 11 10 9 8 7 6 5 4 3 2 1 0
168 hrs.
144 hrs.
120 hrs.
96 hrs.
72 hrs.
48 hrs.
24 hrs.
12 hrs.
8 hrs.
6 hrs.
3 hrs.
1 hr.
PS-34
PS-182
PS-527

Figure 3. Time-resolved ^{1}H NMR spectra of (a) PS-34 at A:S=1:1, (b) PS-182 at A:S=1:1, (c) PS-527 at A:S=1:1, (d) PS-34 at A:S=3:1, (e) PS-182 at A:S=3:1, and (d) PS-527 at A:S=3:1. Stars (*) marks the benzene peaks. The NMR spectra show that the triflic acid generates only benzene from polystyrene in the A:S=1:1 solutions over the 168 hour reaction period but starts to form small molecular weight compounds in the A:S=3:1 after 24 hours.

In the A:S=1:1 solutions, the molecular weights of PS chains increase further at the same reaction time, but the PS chains start to develop low-molecular weight shoulders as marked with the red arrows (figures 2d, 2e, and 2f). The time-resolved ^{1}H NMR spectra are recorded nearly the same except for the increase of benzene peak at 7.37 ppm marked with stars (Figure 3a, 3b, and 3c).

In contrast, the PS solutions of the A:S=3:1 of the highest triflic acid ratio show different behaviors. The PS chromatograms of the A:S=3:1 solution record the decrease of the molecular weights with negligible *inter*-chain coupling signatures (Figures 2g, 2h, and 2i. The potential origin of the chain-coupling mode by the concentration of triflic acid is described below). Three distinct stages in the molecular weight decrease are noticed. In the first stage, the molecular weights barely change, but this period of dormancy depends on the molecular weight (Figure 4a). In the PS-34 solution, the molecular weight stays nearly the same for the first 12 hours, and in the PS-182 and PS-527 solutions, 6 hours. We attribute this difference in dormancy periods to the coil overlap concentration c^*. The polymer chains of longer PS-182 and PS-527 overlap in the solutions, and the activated carbocation sites of those chains couple by a shorter chain translation than the translation distance for PS-34 chain coupling.

In the second stage, the molecular weights decrease with dispersity broadening. However, the dispersities of chains increase up to ~ 1.90 and then decrease as the molecular weights approach

their terminal molecular weights, ~ 3 kg/mol for PS-34 and PS-182 at 48 hours and ~ 10 kg/mol for PS-527 at 96 hours, which are marked with blue arrows in figures 2g, 2h, and 2i (the dispersities at the reaction hours are summarized in Table S1). In the ^{1}H NMR spectra, the peak area ratio of the H^{o} and $H^{m/p}$ of styrene phenyl groups gradually decreases from the initial ratio of styrene monomer, $H^{o}(2)/H^{m/p}(3) = 0.67$ (Figure 4b). With the formation of benzene as shown in the ^{1}H NMR (Figures 3d, 3e, and 3f) and the GC-MS analysis result (see below), the change of H^{o} to $H^{m/p}$ ratio suggests the transformation of styrene to indan units (Scheme 1). This transformation also results in the broad resonance of backbone hydrogens, which reflects increased heterogeneity in chemical environments by indanization and also coupling (Figure S3. See the NMR characterization section in the Supporting Information). The fraction of styrene units in poly(styrene-*co*-indan) chains based on the peak areas are summarized in Figure 4c.[34]

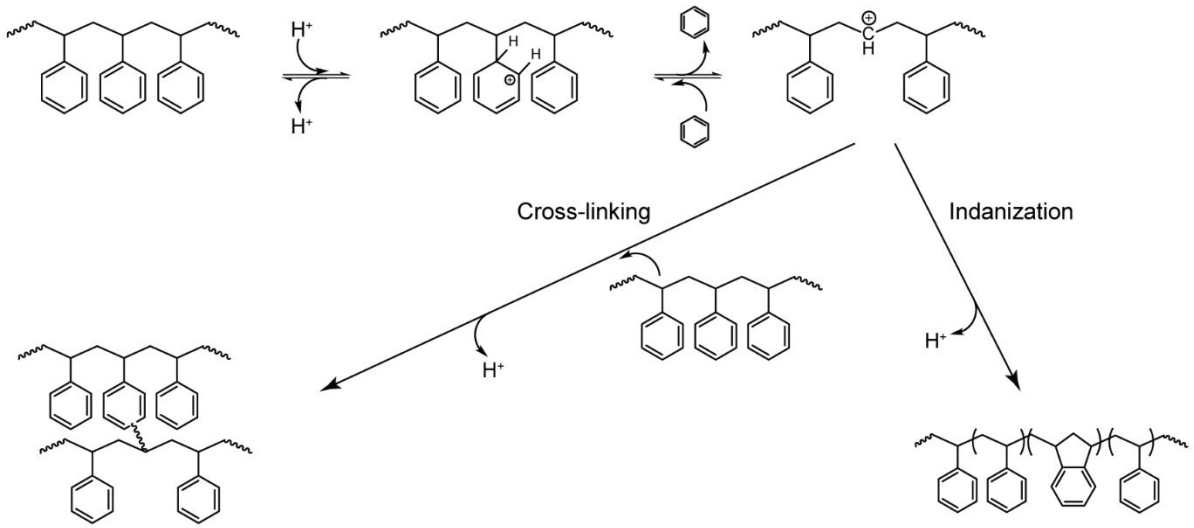

Scheme 1. Crosslinking and indanization reactions activated by the acid-assisted removal of a phenyl group from polystyrene. Crosslinking reactions occur through the *inter*- or *intra*-chain mode depending on the triflic acid concentration.

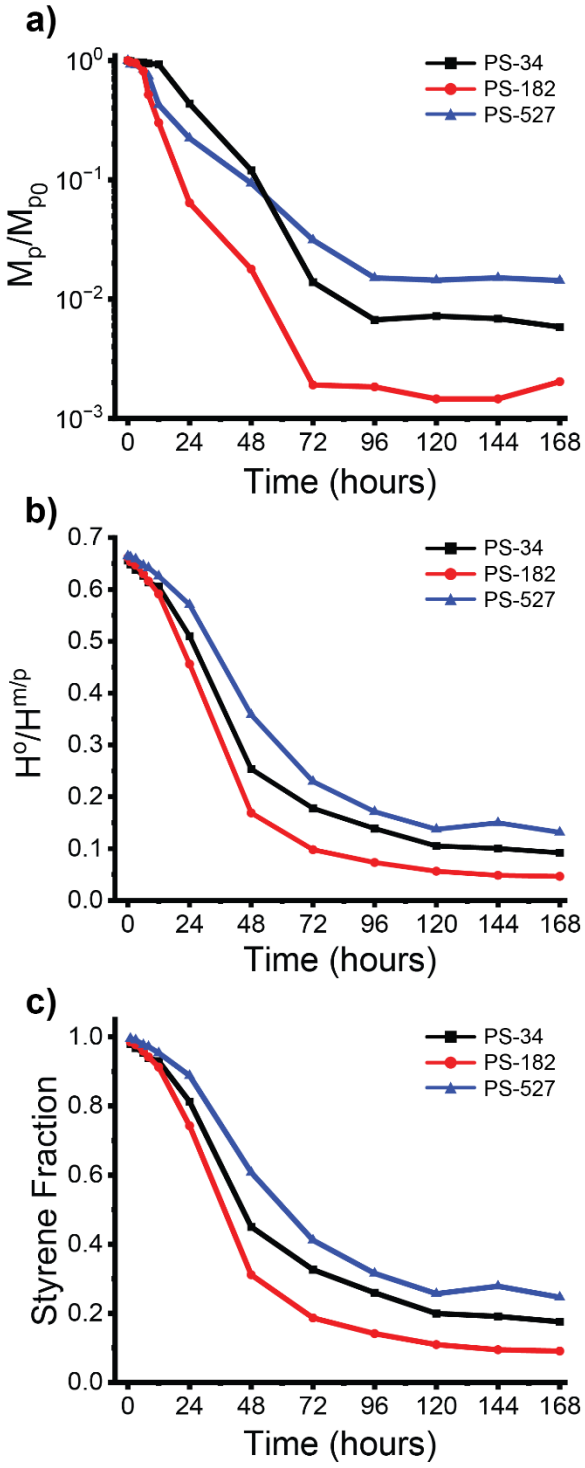
a)
PS-34
PS-182
PS-527
M_p/M_{p0}
10^0
10^{-1}
10^{-2}
10^{-3}
0 24 48 72 96 120 144 168
Time (hours)
b)
PS-34
PS-182
PS-527
$H^o/H^{m/p}$
0.0 0.1 0.2 0.3 0.4 0.5 0.6 0.7
0 24 48 72 96 120 144 168
Time (hours)
c)
PS-34
PS-182
PS-527
Styrene Fraction
0.0 0.2 0.4 0.6 0.8 1.0
0 24 48 72 96 120 144 168
Time (hours)

Figure 4. Changes of the A:S=3:1 solutions over the reaction hours in (a) the nominal peak molecular weights of PS chains, i.e, nanoparticles by *intra*-chain crosslinking, by the chromatography data of Figure 2g, 2h, and 2i, (b) the peak integration ratio of ortho to meta/para hydrogens in the phenyl groups based on the ^{1}H NMR spectra of Figure 3d, 3e, and 3f, and (c) the fraction of styrene units in the poly(styrene-*co*-indan) copolymers based on the ortho to meta/para hydrogen ratios of panel b.

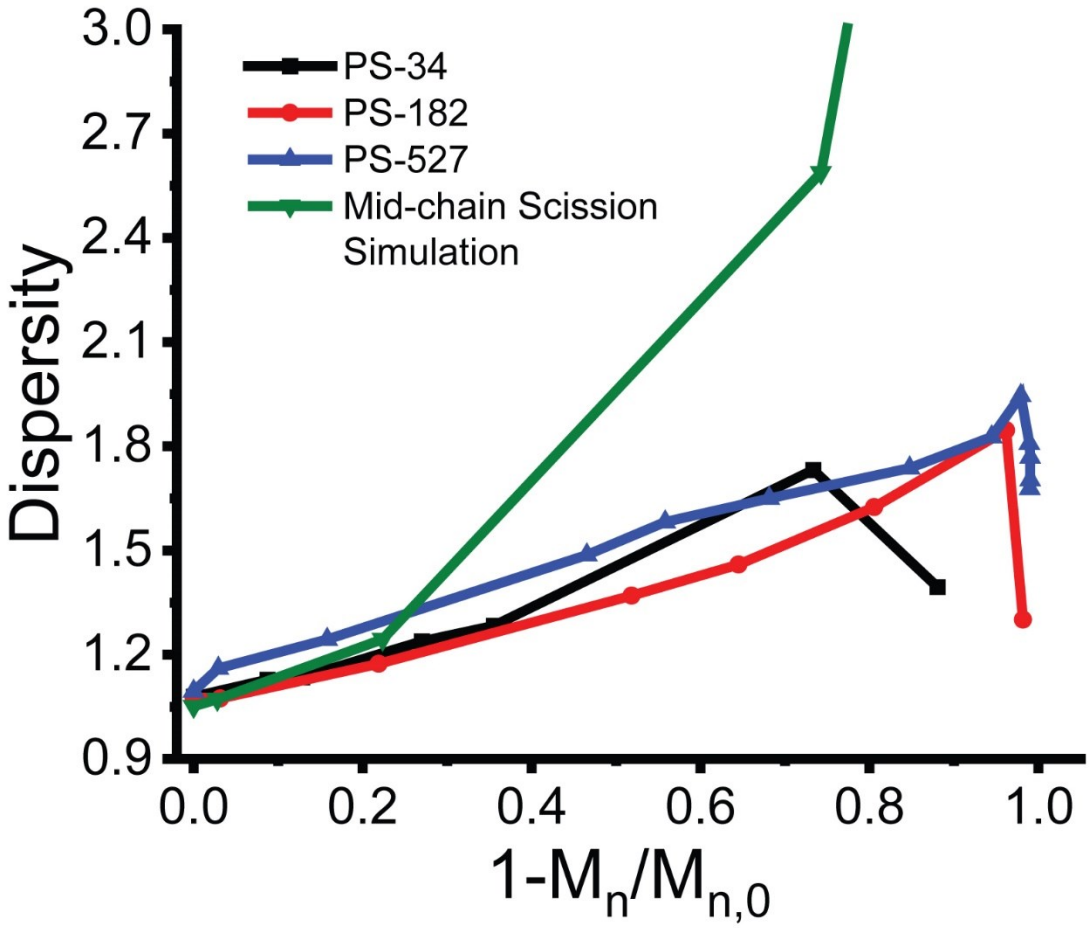

Figure 5. Changes of the PS chain dispersity in the A:S=3:1 solution and simulated chain dispersity as a function of the normalized molecular weight, $1-M_n/M_{n,0}$ where M_n is the number-average molecular weight by the mid-chain scission and $M_{n,0}$ is the initial molecular weight by the mid-chain scission mode. The dispersity of PS chains reacting with triflic acid increases and decreases as the molecular weights reach their terminal molecular values. In contrast, the simulated dispersity by the mid-chain scission mode continues to increase as the molecular weight decreases. The dispersities of PS samples are calculated over the low molecular weight foot of the terminal molecular weight peaks and above.

We considered two potential chemical pathways for the observed molecular weight decrease of PS chains in the A:S=3:1 solution: the depolymerization at the chain ends and the mid-chain scission. However, neither the chain-end depolymerization or the mid-chain scission mode explains the decrease of PS molecular weights by triflic acid. For the chain-end depolymerization, the depolymerized products, monomer or small molecular weight compounds, should be observed, but the first 24 hour ^{1}H NMR spectra do not contain any signs of such new resonance signatures except for benzene despite the nominal molecular weight decrease of the PS samples are evident in the chromatograms (Figure 3d, 3e, and 3f). The mid-chain scission mode neither justifies the observed molecular weight changes because the dispersity of polymer chains by the mid-chain scissions must keep increasing as the chains break down, as our simulation results show in Figure S4. The PS dispersities of the A:S=3:1 solution initially increase and eventually decrease as the nominal molecular weights of PS chains approach the terminal values (Figure 5 and Table S1. In the evaluation of the dispersities of nanoparticles based on nominal molecular weights, the intensity contribution of small molecular weight compounds lower than ~ 500 g/mol, which are marked with blue arrows in Figure 2g, 2h, and 2i, are excluded). Therefore, the mid-chain scission mode also cannot explain the terminal molecular weights observed before the polymer chains break into small compounds (Figures 2g, 2h and 2i).

The inconsistency with those chain degradation modes and the *inter*-chain coupling observed at the low triflic acid concentrations suggest that the molecular weight decrease of the PS of the A:S=3:1 solution in the first 24 hours primarily originates from changes in the chain topology by *intra*-chain couplings which form a crosslinked local network of a polymer chain, i.e., swollen nanoparticle with a reduced hydrodynamic volume.[46-49] This conclusion is consistent with the stable ^{1}H NMR spectra of the PS chains in the first 24 hours despite the large changes in the

nominal molecular weights. It also aligns with the terminal molecular weight behavior of the polymer chains before a relatively large amount of small molecular weight compounds starts to form at 48 hours and later. As the *intra*-chain coupling reactions occur, the hydrodynamic volume decreases. When nearly all conformationally feasible *intra*-chain coupling sites have reacted, the decrease of hydrodynamic volume, i.e., nominal molecular weight, reaches the terminal molecular weight observed in Figures 2g, 2h, and 2i. The decrease of dispersity as the molecular weights approach the terminal values also supports this explanation. In the chromatograms of PS-527 (Figure 2i), the high molecular weight side marked with the red arrow shifts to the lower side as the reaction proceeds, but the lower molecular weight side marked with the green arrow stays the same because the degrees of *intra*-chain crosslinking of individual chains saturate. The reaction pathways forming chain coupling, along with the transformation of styrene to indan unit, by the acid-assisted removal of phenyl groups is described in Scheme 1.

In the third stage (≥ 48 hours), the intensity of the terminal molecular weight peaks decreases, but the terminal molecular weights remain the same while the lower molecular weight products are produced, as marked with diagonal arrows in Figures 2g, 2h, and 2i. This discontinuous shift in molecular weights contrasts the continuous decrease of molecular weights in the second stage by *intra*-chain coupling. The time-resolved ^{1}H-NMR spectra reveal new chemical functional groups forming in this stage (Figure 3d, 3e, and 3f at 48 hours and later). Those observations indicate that the crosslinked polystyrene-*co*-indan nanoparticles break down once activated, and the activation is relatively slow compared to the breaking down rate of an activated chain into small compounds.

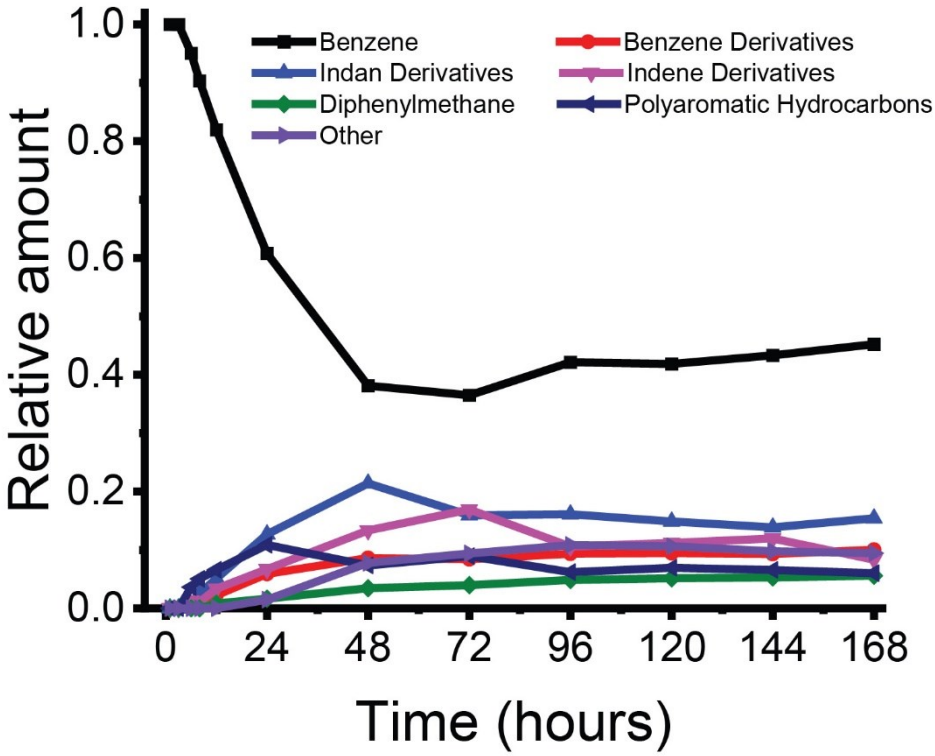

Figure 6. Fraction of small molecular weight compounds produced by reacting PS-182 with three molar equivalent triflic acids (A:S=3:1). The fractions are based on the peak areas of the GC-MS spectra, and the detailed compound compositions are listed in Table S2.

The GC-MS analysis of the PS-182 solutions at the A:S=3:1 reveals a series of small molecular weight compounds (Figure 6). In the first and second stages (≤ 24 hours), benzene is the major compound though the amount of benzene is small in the first hours as shown in the ^{1}H NMR spectrum (Figure 3e). In the third stage (≥ 48 hours), crosslinked polymer nanoparticles start to break, and alkylbenzene isomers, indan/indene derivatives, diphenylmethane, and polycyclic aromatic hydrocarbons form, though benzene is still the major compound.[50, 51] The relative composition of those compounds saturates at ~ 96 hours, but the reaction solution becomes darker by the increasing amount of polycyclic aromatic hydrocarbons (PAHs) such as pyrene and

phenanthrene derivatives (Figure S5).[52, 53] We attribute the PAH formation to the Scholl reactions by triflic acid which serves as a strong Brønsted acid for the reaction.[54-56] The PS-182 samples of the A:S=3:1 solution are characterized using X-ray scattering measurements to check if any crystalline domains exist, but no diffraction signatures are identified (Figure S6. The detail of the scattering experiment is described in the supporting information).

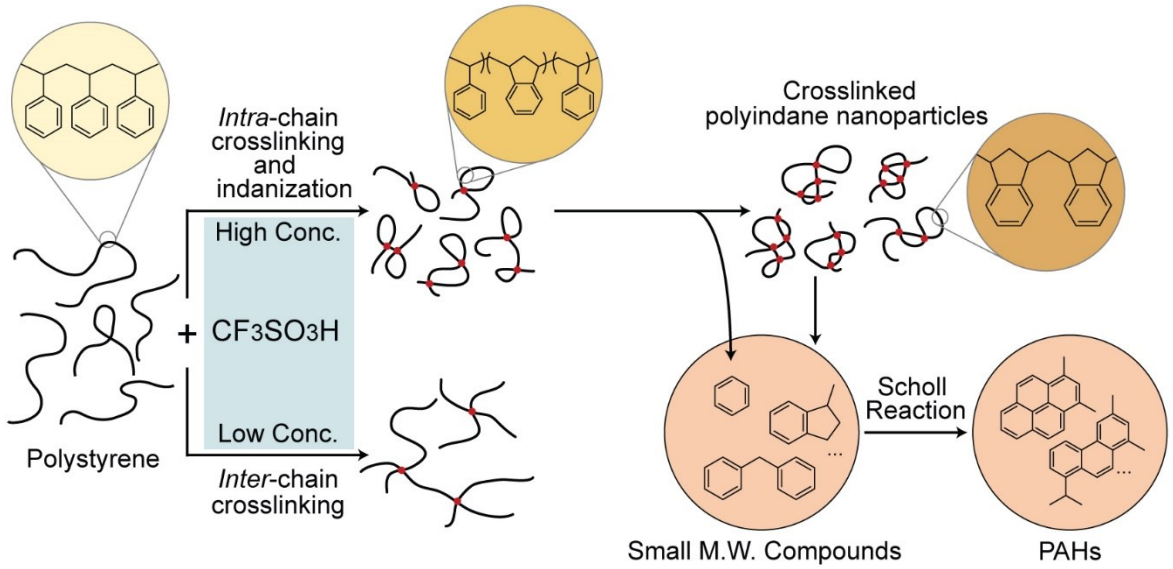

Figure 7. Schematic description of the low-temperature PS chain degradation process by triflic acid. Depending on the relative concentration of triflic acid, the PS chains form *inter*- or *intra*-chain crosslinking. Transformation of styrene units in the chains to indan also occurs while *intra*-chain crosslinking proceeds. The *intra*-chain crosslinked polymer nanoparticles break down into small phenyl-containing compounds, further transforming into polycyclic aromatic hydrocarbons by the Scholl reaction.

Figure 7 summarizes the degradation stages of PS and key characteristics induced by triflic acid observed in this study. Depending on the relative molar ratio of triflic acid to the styrene unit polymerized, we observed the mode of PS coupling changes between *inter*- and *intra*-chain. We speculate that this concentration dependence is related to the formation of ionic group aggregates.[57] In a high triflic acid concentration such as A:S=3:1, multiple parts in a chain may form carbocations which ionically aggregate, and the aggregate compacts the chain conformations for the *intra*-chain coupling despite the conformational entropic penalty. In contrast, in the low triflic acid concentration, the *intra*-chain coupling is less preferred than the *inter*-chain coupling due to the conformational penalty of chains. The chain coupling reaction simultaneously proceeds with the transformation of styrene units to indan because both reactions appear to be activated by the removal of a phenyl group (Scheme 1). Once the *intra*-chain crosslinking completes, the crosslinked polystyrene-*co*-indan nanoparticles break down into small molecules such as benzene, diphenylmethane, and indan/indene derivates, which react with each other and form PAHs such as pyrene and phenanthrene compounds.

Conclusion

Superacid-assisted degradation of PS chains at 20 °C is investigated using time-resolved characterizations. We found that the removal of phenyl groups by acid from linear PS chains induces two key transformations: i) topology changes of PS chains by *inter*- and *intra*-crosslinking and ii) transformation of styrene units to indanes. In the high acid concentration environment, the *intra*-chain crosslinking becomes dominant, crosslinked polymer nanoparticles form, and the crosslinked polymer nanoparticles break down into small compounds. Triflic acid also induces the formation of polycyclic aromatic hydrocarbons from small compounds by the Scholl reaction. This finding shows that the super acid-assisted polymer degradation process at a low temperature

proceeds through distinct stages, which may help establish efficient and economically viable upcycling of end-of-life PS products. For example, temporal control of the polystyrene degradation stages using two catalysts with different activities may enable to separate the indanization step producing benzene from the rest reactions, and controlled breakdown of the crosslinked poly(styrene-co-indan) chains is achieved for value products without PAHs or with value PAHs in the least energy-intensive low-temperature environment as employed in this work.

ASSOCIATED CONTENT

Supporting Information

The following file is available free of charge.

^{1}H NMR characterization data, molecular weight simulation by the chain scission mode, X-ray scattering characterization, dispersity index data, GC-MS characterization data, and photographs of solutions.

AUTHOR INFORMATION

Corresponding Author

Sangwoo Lee - *Department of Chemical and Biological Engineering, Rensselaer Polytechnic Institute, Troy, New York 12180, United States;* Email - lees27@rpi.edu

Authors

Atharwa Thigale - *Department of Chemical and Biological Engineering, Rensselaer Polytechnic Institute, Troy, New York 12180, United States*

Carrie Trant - *Department of Chemical and Biological Engineering, Rensselaer Polytechnic Institute, Troy, New York 12180, United States*

Juhong Ahn - *Department of Chemical and Biological Engineering, Rensselaer Polytechnic Institute, Troy, New York 12180, United States*

Melissa Nelson - *Department of Chemical and Biological Engineering, Rensselaer Polytechnic Institute, Troy, New York 12180, United States*

Chang Y. Ryu - *Department of Chemistry and Chemical Biology, Rensselaer Polytechnic Institute, Troy, New York 12180, United States*

Chulsung Bae - *Department of Chemical and Biological Engineering, Rensselaer Polytechnic Institute, Troy, New York 12180, United States; Department of Chemistry and Chemical Biology, Rensselaer Polytechnic Institute, Troy, New York 12180, United States*

Sangwoo Lee - *Department of Chemical and Biological Engineering, Rensselaer Polytechnic Institute, Troy, New York 12180, United States*

Author Contributions

The manuscript was written through contributions of all authors. All authors have given approval to the final version of the manuscript.

Notes

The authors declare no competing financial interest.

ACKNOWLEDGMENT

This work is supported by the National Science Foundation under Award Number DMR-2029765. This research used resources of the 12-ID beamline of the National Synchrotron Light Source II, a U.S. Department of Energy (DOE) Office of Science User Facility operated for the DOE Office of Science by Brookhaven National Laboratory under Contract No. DESC0012704.

REFERENCES

(1) Geyer, R.; Jambeck, J. R.; Law, K. L. Production, use, and fate of all plastics ever made. *Sci. Adv.* **2017**, *3* (7), e1700782.

(2) Lock, E. H.; Petrovykh, D. Y.; Mack, P.; Carney, T.; White, R. G.; Walton, S. G.; Fernsler, R. F. Surface Composition, Chemistry, and Structure of Polystyrene Modified by Electron-Beam-Generated Plasma. *Langmuir* **2010**, *26* (11), 8857-8868.

(3) Edwards, K. L. A designers' guide to engineering polymer technology. *Mater. Des.* **1998**, *19* (1), 57-67.

(4) Otake, Y.; Kobayashi, T.; Asabe, H.; Murakami, N.; Ono, K. Biodegradation of low-density polyethylene, polystyrene, polyvinyl chloride, and urea formaldehyde resin buried under soil for over 32 years. *J. Appl. Polym. Sci.* **1995**, *56* (13), 1789-1796.

(5) Gautam, R.; Bassi, A. S.; Yanful, E. K. A review of biodegradation of synthetic plastic and foams. *Appl. Biochem. Biotechnol.* **2007**, *141* (1), 85-108.

(6) Schellenberg, J.; Leder, H.-J. Syndiotactic polystyrene: Process and applications. *Adv. Polym. Technol.* **2006**, *25* (3), 141-151.

(7) Scheirs, J.; Priddy, D. B. *Modern styrenic polymers : polystyrenes and styrenic copolymers*; Wiley, 2003.

(8) Miller, R. R.; Newhook, R.; Poole, A. Styrene Production, Use, and Human Exposure. *Crit. Rev. Toxicol.* **1994**, *24* (sup1), S1-S10.

(9) Schyns, Z. O. G.; Shaver, M. P. Mechanical Recycling of Packaging Plastics: A Review. *Macromol. Rapid Commun.* **2021**, *42* (3), 2000415.

(10) Torres, N.; Robin, J. J.; Boutevin, B. Study of thermal and mechanical properties of virgin and recycled poly(ethylene terephthalate) before and after injection molding. *Eur. Polym. J.* **2000**, *36* (10), 2075-2080.

(11) Tournier, V.; Topham, C. M.; Gilles, A.; David, B.; Folgoas, C.; Moya-Leclair, E.; Kamionka, E.; Desrousseaux, M. L.; Texier, H.; Gavalda, S.; et al. An engineered PET depolymerase to break down and recycle plastic bottles. *Nature* **2020**, *580* (7802), 216-219.

(12) Vogt, B. D.; Stokes, K. K.; Kumar, S. K. Why is Recycling of Postconsumer Plastics so Challenging? *ACS Appl. Polym. Mater.* **2021**, *3* (9), 4325-4346.

(13) Korley, L. T. J.; Epps, T. H.; Helms, B. A.; Ryan, A. J. Toward polymer upcycling-adding value and tackling circularity. *Science* **2021**, *373* (6550), 66-69.

(14) Achilias, D. S.; Kanellopoulou, I.; Megalokonomos, P.; Antonakou, E.; Lappas, A. A. Chemical Recycling of Polystyrene by Pyrolysis: Potential Use of the Liquid Product for the Reproduction of Polymer. *Macromol. Mater. Eng.* **2007**, *292* (8), 923-934.

(15) Lin, R.; White, R. L. Acid-catalyzed cracking of polystyrene. *J. Appl. Polym. Sci.* **1997**, *63* (10), 1287-1298.

(16) Audisio, G.; Bertini, F.; Beltrame, P. L.; Carniti, P. Catalytic degradation of polymers: Part III—Degradation of polystyrene. *Polym. Degrad. Stab.* **1990**, *29* (2), 191-200.

(17) Qureshi, M. S.; Oasmaa, A.; Pihkola, H.; Deviatkin, I.; Tenhunen, A.; Mannila, J.; Minkkinen, H.; Pohjakallio, M.; Laine-Ylijoki, J. Pyrolysis of plastic waste: Opportunities and challenges. *J. Anal. Appl. Pyrolysis* **2020**, *152*, 104804.

(18) Peng, B.-Y.; Su, Y.; Chen, Z.; Chen, J.; Zhou, X.; Benbow, M. E.; Criddle, C. S.; Wu, W.-M.; Zhang, Y. Biodegradation of Polystyrene by Dark (*Tenebrio obscurus*) and Yellow (*Tenebrio molitor*) Mealworms (Coleoptera: Tenebrionidae). *Environ. Sci. Technol.* **2019**, *53* (9), 5256-5265.

(19) Yang, Y.; Yang, J.; Wu, W.-M.; Zhao, J.; Song, Y.; Gao, L.; Yang, R.; Jiang, L. Biodegradation and Mineralization of Polystyrene by Plastic-Eating Mealworms: Part 1. Chemical and Physical Characterization and Isotopic Tests. *Environ. Sci. Technol.* **2015**, *49* (20), 12080-12086.

(20) Wang, Z.; Xin, X.; Shi, X.; Zhang, Y. A polystyrene-degrading Acinetobacter bacterium isolated from the larvae of *Tribolium castaneum*. *Sci. Total Environ.* **2020**, *726*, 138564.

(21) Woo, S.; Song, I.; Cha, H. J. Fast and Facile Biodegradation of Polystyrene by the Gut Microbial Flora of *Plesiophthalmus davidis* Larvae. *Appl. Environ. Microbiol.* **2020**, *86* (18), e01361-01320.

(22) Zhang, Y.; Pedersen, J. N.; Eser, B. E.; Guo, Z. Biodegradation of polyethylene and polystyrene: From microbial deterioration to enzyme discovery. *Biotechnol. Adv.* **2022**, *60*, 107991.

(23) Taghavi, N.; Udugama, I. A.; Zhuang, W.-Q.; Baroutian, S. Challenges in biodegradation of non-degradable thermoplastic waste: From environmental impact to operational readiness. *Biotechnol. Adv.* **2021**, *49*, 107731.

(24) Feng, H.-M.; Zheng, J.-C.; Lei, N.-Y.; Yu, L.; Kong, K. H.-K.; Yu, H.-Q.; Lau, T.-C.; Lam, M. H. W. Photoassisted Fenton Degradation of Polystyrene. *Environ. Sci. Technol.* **2011**, *45* (2), 744-750.

(25) Li, Y.; Li, J.; Ding, J.; Song, Z.; Yang, B.; Zhang, C.; Guan, B. Degradation of nano-sized polystyrene plastics by ozonation or chlorination in drinking water disinfection processes. *Chem. Eng. J.* **2022**, *427*, 131690.

(26) Cao, R.; Zhang, M.-Q.; Hu, C.; Xiao, D.; Wang, M.; Ma, D. Catalytic oxidation of polystyrene to aromatic oxygenates over a graphitic carbon nitride catalyst. *Nat. Commun.* **2022**, *13* (1), 4809.

(27) Yue, Q.; Luo, L. Turning trash into treasure: Metal-free upcycling of polystyrene plastic waste to aromatics. *Chem* **2022**, *8* (9), 2326-2329.

(28) Skolia, E.; Mountanea, O. G.; Kokotos, C. G. Photochemical upcycling of polystyrene plastics. *Trends Chem.* **2023**, *5* (2), 116-120.

(29) Li, T.; Vijeta, A.; Casadevall, C.; Gentleman, A. S.; Euser, T.; Reisner, E. Bridging Plastic Recycling and Organic Catalysis: Photocatalytic Deconstruction of Polystyrene via a C–H Oxidation Pathway. *ACS Catal.* **2022**, *12* (14), 8155-8163.

(30) Oh, S.; Stache, E. E. Chemical Upcycling of Commercial Polystyrene via Catalyst-Controlled Photooxidation. *J. Am. Chem. Soc.* **2022**, *144* (13), 5745-5749.

(31) Zhang, G.; Zhang, Z.; Zeng, R. Photoinduced FeCl3-Catalyzed Alkyl Aromatics Oxidation toward Degradation of Polystyrene at Room Temperature†. *Chin. J. Chem.* **2021**, *39* (12), 3225-3230.

(32) Wang, M.; Wen, J.; Huang, Y.; Hu, P. Selective Degradation of Styrene-Related Plastics Catalyzed by Iron under Visible Light. *ChemSusChem* **2021**, *14* (22), 5049-5056.

(33) Huang, Z.; Shanmugam, M.; Liu, Z.; Brookfield, A.; Bennett, E. L.; Guan, R.; Vega Herrera, D. E.; Lopez-Sanchez, J. A.; Slater, A. G.; McInnes, E. J. L.; et al. Chemical Recycling of Polystyrene to Valuable Chemicals via Selective Acid-Catalyzed Aerobic Oxidation under Visible Light. *J. Am. Chem. Soc.* **2022**, *144* (14), 6532-6542.

(34) Nanbu, H.; Sakuma, Y.; Ishihara, Y.; Takesue, T.; Ikemura, T. Catalytic degradation of polystyrene in the presence of aluminum chloride catalyst. *Polym. Degrad. Stab.* **1987**, *19* (1), 61-76.

(35) Xu, Z.; Pan, F.; Sun, M.; Xu, J.; Munyaneza, N. E.; Croft, Z. L.; Cai, G. G.; Liu, G. Cascade degradation and upcycling of polystyrene waste to high-value chemicals. *Proc Natl Acad Sci U S A* **2022**, *119* (34), e2203346119.

(36) Zhang, Z.; Li, D.; Wang, J.; Jiang, J. Cascade upcycling polystyrene waste into ethylbenzene over Fe2N @ C. *Appl. Catal. B* **2023**, *323*, 122164.

(37) Pukánszky, B.; Kennedy, J. P.; Kelen, T.; Tüdős, F. Cationic reactions in the melt. *Polym. Bull.* **1981**, *5* (8), 469-476.

(38) Ojha, D. K.; Vinu, R. Resource recovery via catalytic fast pyrolysis of polystyrene using zeolites. *J. Anal. Appl. Pyrolysis* **2015**, *113*, 349-359.

(39) Kim, J.-S.; Lee, W.-Y.; Lee, S.-B.; Kim, S.-B.; Choi, M.-J. Degradation of polystyrene waste over base promoted Fe catalysts. *Catal. Today* **2003**, *87* (1), 59-68.

(40) Zhang, Z.; Hirose, T.; Nishio, S.; Morioka, Y.; Azuma, N.; Ueno, A.; Ohkita, H.; Okada, M. Chemical recycling of waste polystyrene into styrene over solid acids and bases. *Ind. Eng. Chem. Res.* **1995**, *34* (12), 4514-4519.

(41) Zmierczak, W.; Xiao, X.; Shabtai, J. Depolymerization-liquefaction of plastics and rubbers. 2. Polystyrenes and styrene-butadiene copolymers. *Fuel Process. Technol.* **1996**, *49* (1), 31-48.

(42) Tae, J.-W.; Jang, B.-S.; Kim, J.-R.; Kim, I.; Park, D.-W. Catalytic degradation of polystyrene using acid-treated halloysite clays. *Solid State Ion.* **2004**, *172* (1), 129-133.

(43) Lee, S.-Y.; Yoon, J.-H.; Kim, J.-R.; Park, D.-W. Degradation of polystyrene using clinoptilolite catalysts. *J. Anal. Appl. Pyrolysis* **2002**, *64* (1), 71-83.

(44) Marczewski, M.; Kamińska, E.; Marczewska, H.; Godek, M.; Rokicki, G.; Sokołowski, J. Catalytic decomposition of polystyrene. The role of acid and basic active centers. *Appl. Catal. B* **2013**, *129*, 236-246.

(45) Ukei, H.; Hirose, T.; Horikawa, S.; Takai, Y.; Taka, M.; Azuma, N.; Ueno, A. Catalytic degradation of polystyrene into styrene and a design of recyclable polystyrene with dispersed catalysts. *Catal. Today* **2000**, *62* (1), 67-75.

(46) Harth, E.; Horn, B. V.; Lee, V. Y.; Germack, D. S.; Gonzales, C. P.; Miller, R. D.; Hawker, C. J. A Facile Approach to Architecturally Defined Nanoparticles via Intramolecular Chain Collapse. *J. Am. Chem. Soc.* **2002**, *124* (29), 8653-8660.

(47) Taylor, S. J.; Storey, R. F.; Kopchick, J. G.; Mauritz, K. A. Poly[(styrene-co-p-methylstyrene)-b-isobutylene-b-(styrene-co-p-methylstyrene)] triblock copolymers. 1. Synthesis and characterization. *Polymer* **2004**, *45* (14), 4719-4730.

(48) Roy, R. K.; Lutz, J.-F. Compartmentalization of Single Polymer Chains by Stepwise Intramolecular Cross-Linking of Sequence-Controlled Macromolecules. *J. Am. Chem. Soc.* **2014**, *136* (37), 12888-12891.

(49) Lyon, C. K.; Prasher, A.; Hanlon, A. M.; Tuten, B. T.; Tooley, C. A.; Frank, P. G.; Berda, E. B. A brief user's guide to single-chain nanoparticles. *Poly. Chem.* **2015**, *6* (2), 181-197.

(50) Csicsery, S. M. Acid catalyzed isomerization of dialkylbenzenes. *J. Org. Chem.* **1969**, *34* (11), 3338-3342.

(51) Roberts, R. M. G. Studies in trifluoromethanesulfonic acid. 2. Kinetics and mechanism of isomerization of xylenes. *J. Org. Chem.* **1982**, *47* (21), 4050-4053.

(52) Williams, P. T.; Horne, P. A.; Taylor, D. T. Polycyclic aromatic hydrocarbons in polystyrene derived pyrolysis oil. *J. Anal. Appl. Pyrolysis* **1993**, *25*, 325-334.

(53) Williams, P. T.; Williams, E. A. Product Composition from the Fast Pyrolysis of Polystyrene. *Environ. Technol.* **1999**, *20* (11), 1109-1118.

(54) Sisto, T. J.; Zakharov, L. N.; White, B. M.; Jasti, R. Towards pi-extended cycloparaphenylenes as seeds for CNT growth: investigating strain relieving ring-openings and rearrangements. *Chem. Sci.* **2016**, *7* (6), 3681-3688, 10.1039/C5SC04218F.

(55) Thamatam, R.; Skraba, S. L.; Johnson, R. P. Scalable synthesis of quaterrylene: solution-phase 1H NMR spectroscopy of its oxidative dication. *Chem. Commun.* **2013**, *49* (80), 9122-9124, 10.1039/C3CC46270F.

(56) Zhang, Y.; Pun, S. H.; Miao, Q. The Scholl Reaction as a Powerful Tool for Synthesis of Curved Polycyclic Aromatics. *Chem. Rev.* **2022**, *122* (18), 14554-14593.

(57) Worsfold, D. J.; Bywater, S. Degree of Association of Polystyryl-, Polyisoprenyl-, and Polybutadienyllithium in Hydrocarbon Solvents. *Macromolecules* **1972**, *5* (4), 393-397.